Hindawi
International Journal of Photoenergy
Volume 2018, Article ID 5927485, 7 pages
https://doi.org/10.1155/2018/5927485

Research Article

Antibacterial Activity of Ag-Doped TiO_2 and Ag-Doped ZnO Nanoparticles

Gebretinsae Yeabyo Nigussie,[1] **Gebrekidan Mebrahtu Tesfamariam**,[1] **Berhanu Menasbo Tegegne**,[1] **Yemane Araya Weldemichel**,[1] **Tesfakiros Woldu Gebreab**,[2] **Desta Gebremedhin Gebrehiwot**,[1] **and Gebru Equar Gebremichel**[3]

[1]*Department of Chemistry, College of Natural and Computational Sciences, Mekelle University, Mekelle, Ethiopia*
[2]*Department of Physics, College of Natural and Computational Sciences, Mekelle University, Mekelle, Ethiopia*
[3]*Department of Biology, College of Natural and Computational Sciences, Mekelle University, Mekelle, Ethiopia*

Correspondence should be addressed to Gebretinsae Yeabyo Nigussie; g.tinsae21@gmail.com

Received 21 December 2017; Revised 26 February 2018; Accepted 13 March 2018; Published 2 May 2018

Academic Editor: P. Davide Cozzoli

We report in this paper antibacterial activity of Ag-doped TiO_2 and Ag-doped ZnO nanoparticles (NPs) under visible light irradiation synthesized by using a sol-gel method. Structural, morphological, and basic optical properties of these samples were investigated using X-ray diffraction (XRD), scanning electron microscopy (SEM), energy dispersive X-ray (EDX) spectrum, and UV-Vis reflectance. Room temperature X-ray diffraction analysis revealed that Ag-doped TiO_2 has both rutile and anatase phases, but TiO_2 NPs only have the anatase phase. In both ZnO and Ag-doped ZnO NPs, the hexagonal wurtzite structure was observed. The morphologies of TiO_2 and ZnO were influenced by doping with Ag, as shown from the SEM images. EDX confirms that the samples are composed of Zn, Ti, Ag, and O elements. UV-Vis reflectance results show decreased band gap energy of Ag-doped TiO_2 and Ag-doped ZnO NPs in comparison to that of TiO_2 and ZnO. Pathogenic bacteria, such as *Staphylococcus aureus*, *Pseudomonas aeruginosa*, and *Escherichia coli*, were used to assess the antibacterial activity of the synthesized materials. The reduction in the viability of all the three bacteria to zero using Ag-doped ZnO occurred at 60 μg/mL of culture, while Ag-doped TiO_2 showed zero viability at 80 μg/mL. Doping of Ag on ZnO and TiO_2 plays a vital role in the increased antibacterial activity performance.

1. Introduction

Currently, nanosized materials are the most advanced type of materials, both in scientific knowledge and in commercial applications. Inorganic nanoparticles (NPs), such as silver, copper, titanium, and zinc, are the most interesting NPs due to their applications and positive impact on pathogenic microorganisms [1–4]. NPs have been studied for many years because of their size-dependent physical and chemical properties. Among NPs, great attention has been shifted to nanooxides [5–7]. NPs have attracted great interest due to their special or specific properties and selectivity, especially in pharmaceutical and biological applications [8]. In laboratory tests with NPs, different microorganisms have been eliminated within minutes of contact with the NPs [9–12]. The application of NPs on bacteria is very important since NPs have a tendency to be in the lowest level and directly enter the food chain of the ecosystem [13, 14].

Recently, special attention has been given to TiO_2 and ZnO NPs due to their unique optical, electrical, and chemical properties. TiO_2 is a tremendous photocatalyst, which is widely used for antibacterial activity due to its high photosensitivity, high efficiency, nontoxic nature, strong oxidizing power, relative cheapness, and chemical stability [15]. ZnO is also a promising photocatalyst and plays a pivotal role in antibacterial activity. In line with this, it is low cost, biocompatible, highly catalytic, and environmental friendly [16, 17].

In order to enhance the photocatalytic activity, intensive interdisciplinary researches have been made on TiO_2 [18–20] and ZnO [21–24]. It is known that photocatalytic activity of NPs depends upon their crystalline structure [19], doping [25], surface area [26], and hydroxyl group [19]. Currently, different researchers are engaged in improving the efficiency of photocatalysts by using metal dopants like Ag which is the most effective due to its high stability and good electrical/thermal conductivity. Furthermore, Ag doping on the surface of metal oxides employed to enhance photocatalytic activity by preventing fast e^--h^+ recombination processes [23, 24, 27, 28]; also, this mechanism could lead to the generation of good antibacterial properties. In this work, Ag-doped TiO_2 and Ag-doped ZnO were synthesized using the sol-gel method, and their antibacterial activity was carefully investigated and discussed.

2. Experimental

2.1. Materials and Methods. High-purity (AR grade) titanium tetrachloride ($TiCl_4$) (Merck, EtOH 99%), silver nitrate ($AgNO_3$), zinc nitrate ($ZnNO_3$), hydrochloric acid (HCl), deionized water (DI), and sodium hydroxide (NaOH) were used as precursors for the preparation of NPs and were acquired from Sigma-Aldrich.

2.2. Synthesis of Nanoparticles. TiO_2 NPs were synthesized using an acid-catalyzed sol-gel process, as described elsewhere [29]. First, 1 mL of $TiCl_4$ was slowly added dropwise to 10 mL EtOH (Merck, 99.8%) under vigorous stirring. A large amount of HCl gas was evolved, and a yellowish solution was formed. The gel was subjected to an oven, and it was dried at 100°C for 24 h. Finally, the white TiO_2 powder was obtained. To obtain nanocrystalline particles, TiO_2 was annealed at 450°C for 4 hours.

Ag-doped TiO_2 was synthesized using1 mL $TiCl_4$ (Merck, 99%) slowly added dropwise to 10 mL EtOH (Merck, 99.8%) under vigorous stirring. $AgNO_3$ was mixed gently with 0.5 mL deionized water (DI). After gelation, the NPs were left to dry at 100°C for 24 hours. In addition, the amorphous TiO_2 transformed to a crystalline structure using a furnace at 450°C for 4 hours.

First, 0.5 M $ZnNO_3$ was dissolved in ethanol, and the reaction mixture was kept under constant stirring for 1 hour until $ZnNO_3$ was completely dissolved. Similarly, in another reaction vessel, 0.5 M of NaOH was dissolved under constant stirring for 1 hour. Then, 0.5 M NaOH was added dropwise to the $ZnNO_3$ solution under vigorous stirring for 45 minutes. The reaction mixture was left for 2 hours after NaOH was completely added. Then, the solution was centrifuged for 10 minutes, the precipitate was dried in an oven at approximately 80°C, and $Zn(OH)_2$ was completely converted into ZnO.

Ag-doped ZnO nanopowder was synthesized using a 0.5 M concentration of $AgNO_3$, which was added to the zinc solution before the NaOH solution, and then, the Ag-doped ZnO NPs were obtained from the $Ag(OH)_2$ precipitate. The powder was calcined at a heating rate of 2°C/min in an air atmosphere for 4 hours at 450°C.

2.3. Characterizations of Ag-TiO_2 and Ag-ZnO Nanoparticles. The phase components of the powder were analyzed using PANalytical X'pert PRO with monochromatic Cu Kα radiation, and the samples were scanned over a range of 20–80°. SEM (JEOL JSM-5610 analysis station SEM) was utilized to examine the shape and cross-sectional morphology. The energy dispersive X-ray (EDX) spectrum was recorded with JEOL JSM-5610 SEM equipped with EDX. The UV-Vis diffuse reflectance spectra were measured using a PerkinElmer Lambda 35 spectrometer which was operated at a wavelength range of 200–800 nm.

2.4. Bacterial Strain and Culture Situations. In this trial, three different characteristic bacterial pathogens were nominated: *Staphylococcus aureus* (*S. aureus*, ATCC29737/NCIM-2901), *Pseudomonas aeruginosa* (*P. aeruginosa*, *PA220*), and *Escherichia coli* (*E. coli*, ATCC 25922). These were grown in 61748 LB Broth (Luria Bertani Broth) medium in a humidified incubator at 37°C with constant agitation overnight. The microorganisms were cultured on a nutrient agar plate for 24 hours and grown aerobically at 37°C.

2.4.1. Antibacterial Activity of Ag-TiO_2 and Ag-ZnO Nanoparticles

(1) Bacterial Cell Growth and Viability Resting. The bacterial growth rate was observed in the presence of Ag-TiO_2 and Ag-ZnO NPs, on the bacteria. *S. aureus*, *P. aeruginosa*, and *E. coli* cultures were gathered in the midexponential growth phase, and the cells were collected using centrifugation at 3000 rpm for 10 min. Directly, the bacterial pellet was washed three times with saline water to clean the pellet of medium constituents. Then, 10 μL of the cell suspensions was mixed with seven different concentrations of Ag-TiO_2 and Ag-ZnO NPs (0 μg/mL, 10 μg/mL, 20 μg/mL, 40 μg/mL, 60 μg/mL, 80 μg/mL, and 100 μg/mL) and incubated at 37°C for 2 h with slight shaking. The mixture was then transferred to 5 mL tubes containing 2 mL MH medium, and the tubes were incubated on a rotary shaker at 180 rpm and 37°C. The antibacterial activity was tested by using 107 CFU/mL and then incubated with concentrations of Ag-TiO_2 and Ag-ZnO for 4 h. Next, 20 μL of a successive 106-fold dilution of each bacterial suspension in sterile deionized water was spread onto agar plates to grow for 24 h at 37°C.

$$\text{Survival\%} = \frac{\text{Colony number of treated bacteria}}{\text{Colony number of control bacteria}} \times 100. \quad (1)$$

3. Results and Discussion

3.1. Material Characterization

3.1.1. X-Ray Diffraction. The XRD pattern of pure TiO_2 and Ag-doped TiO_2 samples is shown in Figure 1. It reveals that the unmodified TiO_2 contains only the anatase phase, and its diffraction peaks are well matching with those of the standard anatase phase of TiO_2 Joint Committee on Powder Diffraction Standard (JCPDS card number 01-071-1167), while Ag-doped TiO_2 exhibited both the anatase and rutile phases (JCPDS card number 4-783). In Figure 1(a, b), the (101)

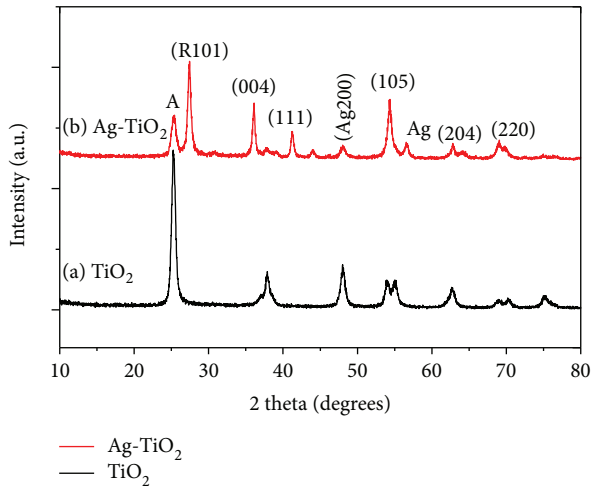

Figure 1: XRD patterns of (a) TiO_2 and (b) Ag-doped TiO_2 nanoparticles.

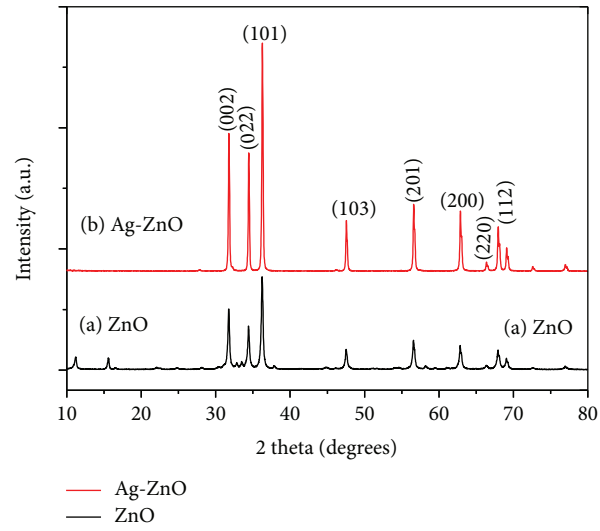

Figure 2: XRD patterns of (a) ZnO and (b) Ag-doped ZnO NPs.

diffraction peak appeared to be attributed to both TiO_2 and Ag-doped TiO_2. Xu et al. [30] reported that a mixture of anatase and rutile phases of Ag-doped TiO_2 possesses greater photocatalytic activity than the pure anatase phase of TiO_2 under UV light. This is evidenced by the presence of Ag in the diffractogram of the Ag-doped samples with the relative intensity of the stronger Ag peaks, (111) at 2θ of 42.500° and (200) at 2θ of 48.500°. Furthermore, this result agrees with that of other reports [31], in which calcination is used to increase the crystallinity of TiO_2 by decreasing the e^--h^+ pair recombination and enhance the photocatalytic activity as well.

Figure 2(a, b) represents the XRD pattern of pure and Ag-doped ZnO collected over a 2θ range of 20°–80° using Cu Kα radiation.

The XRD pattern of the ZnO NP (Figure 2) shows its characteristic peaks with a hexagonal wurtzite structure. The broadening of the graph illustrates the nanometer range of the particle. Our data is in agreement with that of JCPDS card number 36-1451 [1]. The strongest peaks observed at 2θ values of 31.791°, 34.421°, 36.252°, 47.511°, 56.602°, 62.862°, 67.961°, and 69.000° correspond to the lattice planes (100), (002), (101), (110), (103), (112), (201), and (200), respectively. The XRD pattern of Ag-doped ZnO NPs (Figure 2(b)) shows the characteristic peak of Ag at 2θ of 38.110°, 44.270°, and 64.420° (JCPDS card number 04-0783). No shift was observed for ZnO peaks, confirming the surface doping or segregation of Ag nanoclusters on the grain boundaries of ZnO NPs [32].

3.1.2. SEM Analysis. The morphologies of the samples were observed by SEM. Figures 3(a)–3(d) show the morphologies of the samples and Ag distribution in the as-synthesized samples. It can be seen that the surface of Ag in Figures 3(b) and 3(d) is smooth. The nanostructure of the sample as revealed by SEM shows a significant difference in the undoped and doped states. Large elongated grains together with a granular structure show evidence of mixed phases which is in accordance with the XRD results of the corresponding gel powder (Figure 2). These results are in accordance with the values found in the literature [33]. Furthermore, the compositions of the samples were determined with energy dispersive X-ray spectroscopy (EDX) (Figure 4(a, b)). All of the peaks on the curves are recognized to be of Zn, Ag, Ti, O, Cu, C, and Na elements, and no peaks of other elements are observed. The Cu, C, and Na signals might be from the precursors and sample holders. Therefore, it is concluded that the as-synthesized samples are composed of Zn, Ti, Ag, and O elements, which is in good agreement with the above XRD result.

3.1.3. Optical Properties. As shown in Figure 4, Ag-TiO_2 and Ag-ZnO exhibited atypical absorption characteristics due to a band gap change in the range 400–550 nm in the visible region caused by the surface plasmon band characteristics of silver; it was further confirmed that Ag was effectively deposited on the surface of TiO_2 and ZnO [34]. The shift in absorption spectra provides some evidence of the interaction between Ag and TiO_2 or ZnO, which is also in agreement with the XRD patterns.

3.2. Antibacterial Activity of the Nanoparticles. The antibacterial activities of Ag-TiO_2 and Ag-ZnO were examined against gram-positive *S. aureus* and gram-negative *P. aeruginosa* and *E.coli* bacteria, as shown in Figure 5. The Ag-TiO_2 and Ag-ZnO NPs at concentrations of 60 μg/mL of culture were toxic to the three different bacteria tested Figure 5. However, 40 μg/mL concentrations of Ag-ZnO NPs eliminated 100% *P. aeruginosa* cells, whereas 15% and 12% viabilities of *S. aureus* and *E. coli* were obtained, respectively. In Ag-doped NPs at 60 μg/mL of culture, 0% viability in the case of *P. aeruginosa* and *S. aureus* was observed, while in *E. coli*, viabilities were observed. Therefore, here it was determined that 60 μg/mL Ag-doped NP concentration of bacterial culture (0.2 OD at 600 nm) is the optimal concentration for eliminating the bacteria.

When we compare the antibacterial activity of Ag-ZnO NPs to that of Ag-TiO_2 NPs, it was observed that Ag-ZnO

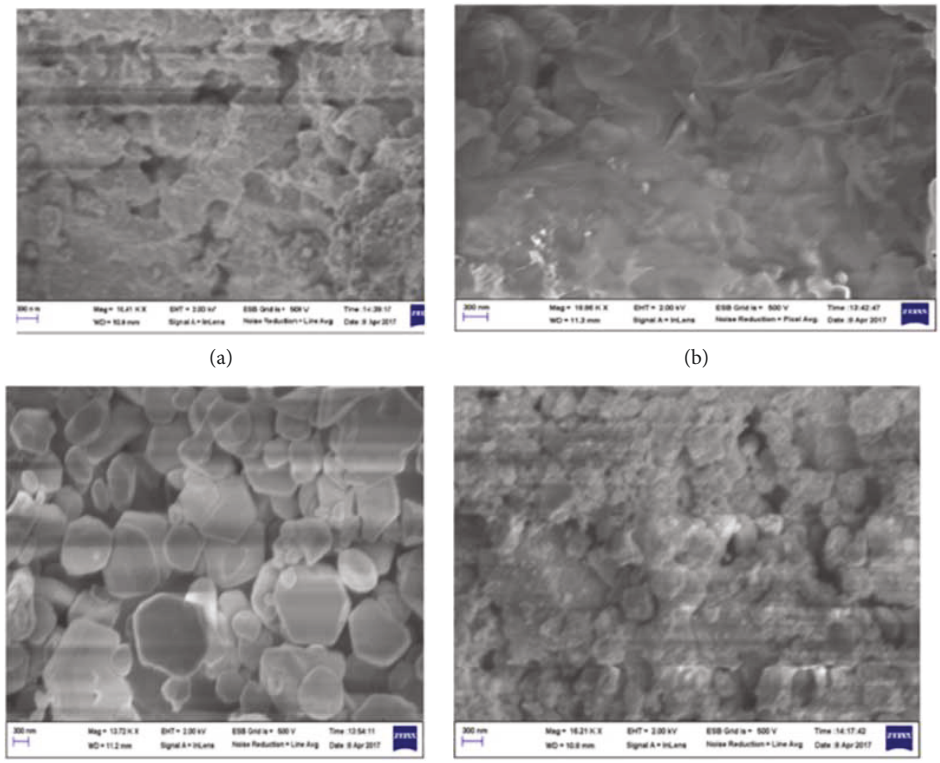

Figure 3: SEM images of (a) pure TiO_2, (b) Ag-TiO_2, (c) pure ZnO, and (d) Ag-ZnO NPs.

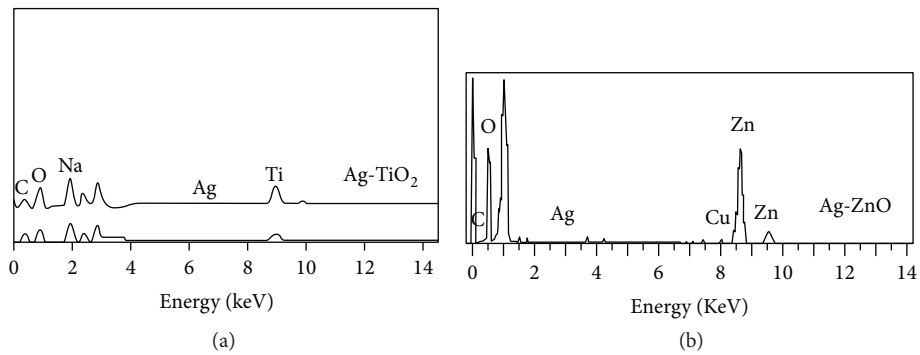

Figure 4: EDX spectrum of (a) Ag-TiO_2 and (b) Ag-ZnO.

NPs are highly efficient. A significant antibacterial activity was observed on gram-negative bacteria in both doped NPs. It may be that gram-positive bacteria have a stronger molecular network in the cell wall than gram-negative bacteria and silver ions may enter the cell walls of gram-positive bacteria [29]. The percent viability of bacteria was exponentially reduced as the concentration of Ag doping increased in the TiO_2 and ZnO matrix. The observed results of this study, along with those of a previous study [35], demonstrate that doping with metal or metal oxide on the surface of TiO_2 and ZnO NPs increases the e^--h^+ charge separation by reducing the band gap energy and leads to a delay in the recombination and an increase in the antibacterial activity Figure 6.

4. Conclusion

In summary, Ag-TiO_2 and Ag-ZnO were prepared via the sol-gel method. The synthesized NPs were characterized using XRD, SEM, EDX, and UV-Vis. This study may provide new insights into the design and preparation of nanomaterials and the enhancement of antibacterial activity. In comparison to other materials, the antibacterial results were more favorable for assays conducted with the same species. Moreover, the low antibacterial activities of pure TiO_2 and ZnO were significantly improved by the incorporation of silver. The synthesized Ag-TiO_2 and Ag-ZnO NPs with high thermal stability and strong antibacterial activity are expected to serve in applications in the

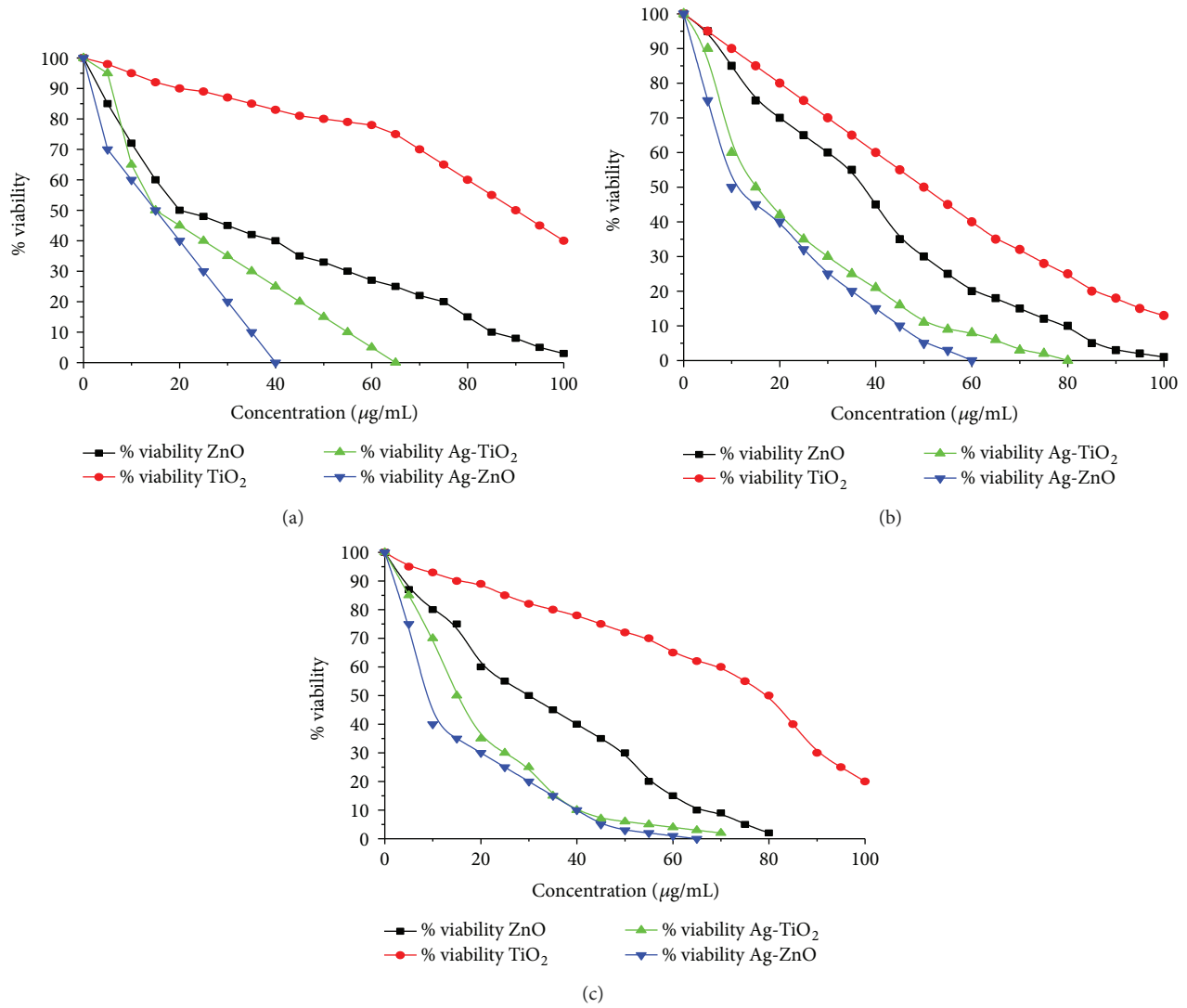

Figure 5: Viability of (a) *P. aeruginosa*, (b) *S. aureus*, and (c) *E. coli* with respect to the concentration of NPs in μg/mL.

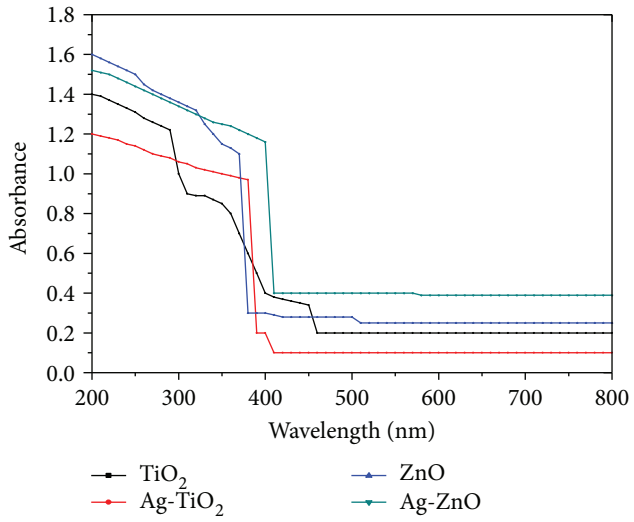

Figure 6: UV-Vis diffuse reflectance spectra of the TiO_2, ZnO, Ag-TiO_2, and Ag-ZnO.

pharmaceutical and nanocomposite fields. Our work provided a possible way to develop nanomaterials with very attractive properties to be applied in antibacterial activities.

Conflicts of Interest

In this, the authors wish to confirm that there are no conflicts of interest associated with this publication.

Acknowledgments

The authors would like to acknowledge Mekelle University for their financial support from the recurrent budget (Grant no. CRPO/CNCS/016/08). They are also grateful to Osmania University, India, and TIGP-SCST for their provision of XRD and SEM analyses.

References

[1] S. Prabhu and E. K. Poulose, "Silver nanoparticles: mechanism of antimicrobial action, synthesis, medical applications, and

toxicity effects," *International Nano Letters*, vol. 2, no. 1, p. 32, 2012.

[2] X. Wan, T. Wang, Y. Dong, and D. He, "Development and application of TiO_2 nanoparticles coupled with silver halide," *Journal of Nanomaterials*, vol. 2014, Article ID 908785, 5 pages, 2014.

[3] S. Chen, Y. Guo, S. Chen, Z. Ge, H. Yang, and J. Tang, "Fabrication of Cu/TiO_2 nanocomposite: toward an enhanced antibacterial performance in the absence of light," *Materials Letters*, vol. 83, pp. 154–157, 2012.

[4] V. Mohammad, A. Umar, and Y. B. Hahn, "ZnO nanoparticles: growth, properties, and applications," in *Metal Oxide Nanostructures and their Applications*, American Scientific Publishers, New York, NY, USA, 2010.

[5] C. B. Murray, C. R. Kagan, and M. G. Bawendi, "Synthesis and characterization of monodisperse nanocrystals and close-packed nanocrystal assemblies," *Annual Review of Materials Research*, vol. 30, no. 1, pp. 545–610, 2000.

[6] L. Cermenati, D. Dondi, M. Fagnoni, and A. Albini, "Titanium dioxide photocatalysis of adamantane," *Tetrahedron*, vol. 59, no. 34, pp. 6409–6414, 2003.

[7] R. Kumar, D. Rana, A. Umar, P. Sharma, S. Chauhan, and M. S. Chauhan, "Ag-doped ZnO nanoellipsoids: potential scaffold for photocatalytic and sensing applications," *Talanta*, vol. 137, pp. 204–213, 2015.

[8] P. Li, J. Li, C. Wu, Q. Wu, and J. Li, "Synergistic antibacterial effects of β-lactam antibiotic combined with silver nanoparticles," *Nanotechnology*, vol. 16, no. 9, pp. 1912–1917, 2005.

[9] T. Sungkaworn, W. Triampo, P. Nalakarn et al., "The effects of TiO_2 nanoparticles on tumor cell colonies: fractal dimension and morphological properties," *International Journal of Biomedical Science*, vol. 2, no. 1, pp. 67–74, 2007.

[10] G. Nagaraju, Udayabhanu, Shivaraj et al., "Electrochemical heavy metal detection, photocatalytic, photoluminescence, biodiesel production and antibacterial activities of Ag–ZnO nanomaterial," *Materials Research Bulletin*, vol. 94, pp. 54–63, 2017.

[11] Y. Xiang, J. Li, X. Liu et al., "Construction of poly(lactic-*co*-glycolic acid)/ZnO nanorods/Ag nanoparticles hybrid coating on Ti implants for enhanced antibacterial activity and biocompatibility," *Materials Science and Engineering: C*, vol. 79, pp. 629–637, 2017.

[12] S. M. Lam, J. A. Quek, and J. C. Sin, "Mechanistic investigation of visible light responsive Ag/ZnO micro/nanoflowers for enhanced photocatalytic performance and antibacterial activity," *Journal of Photochemistry and Photobiology A: Chemistry*, vol. 353, pp. 171–184, 2018.

[13] J. D. Fortner, D. Y. Lyon, C. M. Sayes et al., "C_{60} in water: nanocrystal formation and microbial response," *Environmental Science & Technology*, vol. 39, no. 11, pp. 4307–4316, 2005.

[14] M. Herrera, P. Carrión, P. Baca, J. Liébana, and A. Castillo, "In vitro antibacterial activity of glass-ionomer cements," *Microbios*, vol. 104, no. 409, pp. 141–148, 2001.

[15] A. Kösemen, Z. Alpaslan Kösemen, B. Canimkubey et al., "Fe doped TiO_2 thin film as electron selective layer for inverted solar cells," *Solar Energy*, vol. 132, pp. 511–517, 2016.

[16] H. Morkoç and Ü. Özgür, *Zinc Oxide: Fundamentals, Materials and Device Technology*, Wiley-VCH, Weinheim, Germany, 2009.

[17] J. Jayabharathi, C. Karunakaran, V. Kalaiarasi, and P. Ramanathan, "Nano ZnO, Cu-doped ZnO, and Ag-doped ZnO assisted generation of light from imidazole," *Journal of Photochemistry and Photobiology A: Chemistry*, vol. 295, pp. 1–10, 2014.

[18] L. Elsellami, F. Dappozze, A. Houas, and C. Guillard, "Effect of Ag^+ reduction on the photocatalytic activity of Ag-doped TiO_2," *Superlattices and Microstructures*, vol. 109, pp. 511–518, 2017.

[19] S. Krejčíková, L. Matějová, K. Kočí et al., "Preparation and characterization of Ag-doped crystalline titania for photocatalysis applications," *Applied Catalysis B: Environmental*, vol. 111-112, no. 112, pp. 119–125, 2012.

[20] K. Ubonchonlakate, L. Sikong, and F. Saito, "Photocatalytic disinfection of *P.aeruginosa* bacterial Ag-doped TiO2 film," *Procedia Engineering*, vol. 32, pp. 656–662, 2012.

[21] Y. Zhang, X. Gao, L. Zhi et al., "The synergetic antibacterial activity of Ag islands on ZnO (Ag/ZnO) heterostructure nanoparticles and its mode of action," *Journal of Inorganic Biochemistry*, vol. 130, pp. 74–83, 2014.

[22] Y. Al-Hadeethi, A. Umar, A. A. Ibrahim et al., "Synthesis, characterization and acetone gas sensing applications of Ag-doped ZnO nanoneedles," *Ceramics International*, vol. 43, no. 9, pp. 6765–6770, 2017.

[23] O. Bechambi, M. Chalbi, W. Najjar, and S. Sayadi, "Photocatalytic activity of ZnO doped with Ag on the degradation of endocrine disrupting under UV irradiation and the investigation of its antibacterial activity," *Applied Surface Science*, vol. 347, pp. 414–420, 2015.

[24] M. Elango, M. Deepa, R. Subramanian, and A. Mohamed Musthafa, "Synthesis, characterization of polyindole/Ag—ZnO nanocomposites and its antibacterial activity," *Journal of Alloys and Compounds*, vol. 696, pp. 391–401, 2017.

[25] R. Kumar, J. Rashid, and M. A. Barakat, "Zero valent Ag deposited TiO_2 for the efficient photocatalysis of methylene blue under UV-C light irradiation," *Colloids and Interface Science Communications*, vol. 5, pp. 1–4, 2015.

[26] S. Angkaew and P. Limsuwan, "Preparation of silver-titanium dioxide core-shell (Ag@TiO_2) nanoparticles: effect of Ti-Ag mole ratio," *Procedia Engineering*, vol. 32, pp. 649–655, 2012.

[27] A. Hastir, N. Kohli, and R. C. Singh, "Ag doped ZnO nanowires as highly sensitive ethanol gas sensor," *Materials Today: Proceedings*, vol. 4, no. 9, pp. 9476–9480, 2017.

[28] M. Jakob, H. Levanon, and P. V. Kamat, "Charge distribution between UV-irradiated TiO_2 and gold nanoparticles: determination of shift in the Fermi level," *Nano Letters*, vol. 3, no. 3, pp. 353–358, 2003.

[29] K. Gupta, R. P. Singh, A. Pandey, and A. Pandey, "Photocatalytic antibacterial performance of TiO_2 and Ag-doped TiO_2 against *S. aureus. P. aeruginosa* and *E. coli*," *Beilstein Journal of Nanotechnology*, vol. 4, pp. 345–351, 2013.

[30] H. Xu, H. Li, C. Wu, J. Chu, Y. Yan, and H. Shu, "Preparation, characterization and photocatalytic activity of transition metal-loaded $BiVO_4$," *Materials Science and Engineering: B*, vol. 147, no. 1, pp. 52–56, 2008.

[31] X. You, F. Chen, and J. J. Zhang, "Effects of calcination on the physical and photocatalytic properties of TiO_2 powders prepared by sol–gel template method," *Journal of Sol-Gel Science and Technology*, vol. 34, no. 2, pp. 181–187, 2005.

[32] N. Y. Jamil, S. A. Najim, A. M. Muhammed, and V. M. Rogoz, "Preparation, structural and optical characterization of ZnO/Ag thin film by CVD," *Proceedings of the International*

Conference Nanomaterials: Applications and Properties, vol. 3, no. 2, pp. 32–45, 2014.

[33] B. Cheng, Y. Le, and J. Yu, "Preparation and enhanced photocatalytic activity of Ag@TiO_2 core–shell nanocomposite nanowires," *Journal of Hazardous Materials*, vol. 177, no. 1–3, pp. 971–977, 2010.

[34] C. Chen, Y. Zheng, Y. Zhan, X. Lin, Q. Zheng, and K. Wei, "Enhanced Raman scattering and photocatalytic activity of Ag/ZnO heterojunction nanocrystals," *Dalton Transactions*, vol. 40, no. 37, pp. 9566–9570, 2011.

[35] S. Banerjee, J. Gopal, P. Muraleedharan, A. K. Tyagi, and B. Raj, "Physics and chemistry of photocatalytic titanium dioxide: visualization of bactericidal activity using atomic force microscopy," *Current Science*, vol. 90, no. 10, pp. 1378–1383, 2006.